MEASURING FRACTAL DIMENSION:
MORPHOLOGICAL ESTIMATES AND ITERATIVE OPTIMIZATION

Petros Maragos   and   Fang-Kuo Sun

Division of Applied Sciences
Harvard University
Cambridge, MA 02138

The Analytic Sciences Corp.
55 Walkers Brook Drive
Reading, MA 01867

Abstract

An important characteristic of fractal signals is their fractal dimension. For arbitrary fractals, an efficient approach to evaluate their fractal dimension is the covering method. In this paper we unify many of the current implementations of covering methods by using morphological operations with varying structuring elements. Further, in the case of parametric fractals depending on a parameter that is in one-to-one correspondence with their fractal dimension, we develop an optimization method, which starts from an initial estimate and by iteratively minimizing a distance between the original function and the class of all such functions, spanning the quantized parameter space, converges to the true fractal dimension.

1   Introduction

Fractals are mathematical sets with a high degree of geometrical complexity that can model many natural phenomena [7]. Examples include physical objects such as clouds, mountains, trees and coastlines, as well as image intensity signals that emanate from them (assuming certain restrictions on the object's reflectance and illumination [12]). Although, the fractal images are the most popularized class of fractals due to their fantastic resemblance with natural scenes, there are also numerous natural processes described by time-series measurements (e.g., $1/f$-noises, econometric and demographic data, pitch variations in music signals) that are fractals [7,17]. The one-dimensional *signals* $f(t)$ representing these measurements are fractals in the sense that their graph $G(f) = \{(t, y) : y = f(t)\}$ is a fractal set. Thus, modeling fractal signals is of great interest in signal and image analysis.

An important characteristic of fractals useful for their description and classification is their *fractal dimension* D, which exceeds their topological dimension. Intuitively, D measures the degree of their boundary fragmentation or roughness. It makes meaningful the measurement of metric aspects of fractal sets such as their length or area. Specifically, given a measure unit (a "yardstick") of length ϵ, the length $L(\epsilon)$ of a curve at scale ϵ is equal to the number of yardsticks that can fit sequentially along the curve times ϵ. For a fractal curve, $L(\epsilon)$ increases without limit when ϵ decreases and follows the proportionality law $L(\epsilon) \propto \epsilon^{1-D}$. Taking logarithms yields

$$\log[L(\epsilon)] = (1 - D)\log(\epsilon) + constant \tag{1}$$

Hence, D can be measured from the slope of the $(\log L(\epsilon), \log \epsilon)$ data.

In this paper we deal with the problem of estimating the fractal dimension of "topologically one-dimensional" (1-dim) signals with discrete argument. (Extending most of the ideas in this paper to 2-dim signals is very straightforward and hence omitted.) We start in Section 2.1 and Section 2.2 with a brief survey of some existing methods, some of which are general whereas others apply only to special classes of fractals. Section 2.3 focuses on the *covering method*, a general and efficient approach to compute the fractal dimension of arbitrary fractals. We unify and extend many of the current digital implementations of the

covering method by using morphological erosions and dilations with varying structuring elements. (The erosions and dilations are the basic operators of signal and image analysis by mathematical morphology [13].) We shall refer to these unified algorithms as *morphological estimates*. In addition, to its conceptual usefulness as a unifying theme, the morphological approach has two practical advantages: 1) it reduces the dimensionality of the processed data from two to one, and 2) it is simple to implement. In Section 2.4 we discuss two implementations of the *variation* method for estimating fractal dimension, introduced in [4]. The variation method can be interpreted as stemming from a special case of the morphological approach to implement the covering method.

Both the covering and variation methods apply to arbitrary fractals. However, their actual performance can be tested on parametric fractals, e.g., fractals depending on a single parameter that is in one-to-one correspondence with their fractal dimension D. Fortunately, there are numerous classes of such parametric fractal signals and related algorithms for their synthesis. Two examples used in this paper are the random functions of *fractional Brownian motion (FBM)* [8] and the deterministic *Weierstrass-Mandelbrot cosine (WMC)* functions [2]. Although the performance of the covering and variation method is satisfactory for some cases (i.e., yields reasonable estimation errors), if one is free to vary arbitrarily important parameters of the problem such as D or the signal's duration, then, as our experiments on FBM and WMC functions indicate, their performance falls drastically in many instances. Thus in Section 3 we present the main contribution of this paper, which is both a very effective method (i.e., it yields practically zero estimation errors) to estimate fractal dimension and a new way of looking at this problem. It is somewhat restricted since it applies only to parametric fractals, but the large number of such parametric classes and their practical applicability motivates well our new method. Our basic idea is as follows: So far researchers start from an original fractal signal of true fractal dimension D, use various approaches to derive an estimate, D^*, of D, and are content if the estimation error $|D - D^*|$ is small. This criterion, however, does not say anything about how "close" is the original fractal signal to some other fractal signal of true dimension D^*. Further, any degree of "closeness" should be somehow compatible with laws of visual perception since the fractal dimension is a geometrical attribute. In our approach, from an initial morphological estimate D^* we synthesize the corresponding fractal function f^*. Then by searching in the parameter space D we solve a nonlinear optimization problem, where a distance is iteratively minimized between the original f and each new iteratively synthesized f^*. The process terminates when we reach a local or global minimum. We call this the *Iterative Optimization* method. As distance metrics we have used standard ℓ_p, $p = 1, 2, \infty$, metrics. We also introduced a Hausdorff-type distance for this iterative optimization. Our motivation for using this distance is that it is more suitable than ℓ_p distances to compare two signals in terms of their overall geometrical structure, which is a signal attribute that fractal methods attempt to capture.

Finally we conclude with an application of the above ideas to determine the optimum fractal function for signal interpolation among a parametric class of deterministic fractal functions stemming from the theory of Iterated Function Systems [1].

2 Covering and Variation Methods

2.1 General Methods

Descriptions of various approaches to measure fractal dimension can be found in [7,17,4]. Mandelbrot [7] defines formally the fractal dimension of a set as its Hausdorff-Besicovitsch dimension D_{HB}. Thus, a subset of $\mathbf{R}^E$ is fractal if D_{HB} strictly exceeds its topological dimension D_T. Some very closely related dimensions are the Minkowski-Bouligand dimension D_{MB} [10,3] and the box dimension D_B [3], which are obtained in a different way but are identical; i.e., $D_{MB} = D_B$. In addition, in most cases of practical interest $D_{HB} = D_{MB}$. In this paper we focus on the Minkowski-Bouligand dimension, which we shall henceforth call fractal dimension D, because: 1) it is closely related to D_{HB} and hence able to quantify the

fractal aspects of a signal, 2) it coincides with D_{HB} in many cases; 3) efficient algorithms exist to compute it; 4) it will be applied to discrete signals where most approaches can yield only approximate results.

Let G be a planar curve whose dimension $1 \leq D \leq 2$ is to estimate. Although, $D_B = D_{MB}$ in the continuous case, they correspond to the following two different algorithms (with different performances) in the discrete case.

Box counting method: Partition the plane with squares of side ϵ and count the number $N(\epsilon)$ of squares that intersect the curve. Then $D = \lim_{\epsilon \to 0} \log[N(\epsilon)]/\log(1/\epsilon)$. If an equivalent length $L(\epsilon) = \epsilon N(\epsilon)$ is defined by dividing the total area of these squares by ϵ, then $L(\epsilon)$ behaves as in (1).

Minkowski Cover method: This is based conceptually on Minkowski's idea of finding the length of irregular curves: dilate them with disks of radius ϵ (and thus create a "Minkowski sausage"), find the area $A(\epsilon)$ of the dilated set, and set its length equal to $\lim_{\epsilon \to 0} L(\epsilon)$, where $L(\epsilon) = A(\epsilon)/2\epsilon$. If G is a fractal, then $L(\epsilon)$ behaves as in (1).

Generalized Cover method [4]: This method unifies the box counting and the Minkowski cover method by viewing them as special cases of a generalized "cover". This cover $C(\epsilon)$ is the union of sets B from a family $\mathcal{B}$ such that: $G \subseteq C(\epsilon)$, and each $B \in \mathcal{B}$ intersects G, is homeomorphic to the disk and has diameter on the order of ϵ. If $A(\epsilon)$ is the area of the cover, then it was shown in [16,4] that

$$\log \frac{A(\epsilon)}{\epsilon^2} = D \cdot \log(\frac{1}{\epsilon}) + constant \tag{2}$$

Thus, in all the above methods, D can be estimated by fitting a straight line to and measuring the slope of the plot of the data $(\log L(\epsilon), \log \epsilon)$ or, equivalently, of the data $(\log[A(\epsilon)/\epsilon^2], \log 1/\epsilon)$.

2.2 Parametric Fractals and Special Methods

The FBM and WMC fractal functions are the two primary classes of parametric test signals on which we shall evaluate the various methods.

The FBM $B_H(t)$ with parameter $0 < H < 1$ is a time-varying random function with stationary, Gaussian-distributed, and *statistically self-affine* increments; the latter means that $[B_H(t + T) - B(t)]$ is statistically indistinguishable from $r^{-H}[B(t + rT) - B(t)]$ for any t and any $r > 0$. Their power spectrum is $S(\omega) \propto 1/\omega^{2H+1}$. Hence, an efficient algorithm [17] to synthesize an FBM is to create a random sampled spectrum whose average magnitude is $1/\omega^{H+0.5}$ and its random phase is uniformly distributed over $[0, 2\pi]$. In our experiments we synthesized and then transformed this spectrum via a 2048-point inverse FFT to obtain the FBM sequence from which we retained the first $(N + 1)$ samples.

Another example of parametric fractals is the class of WMC functions

$$W_H(t) = \sum_{n=-\infty}^{\infty} \gamma^{-nH}[1 - \cos(\gamma^n t)] \ , \ 0 < H < 1 \ , \tag{3}$$

where $\gamma > 1$. In our experiments we created WMC sequences by sampling $t \in [0, 1]$ at $(N + 1)$ equidistant points, using a fixed $\gamma = 5$, and by truncating the infinite series so that the remaining finite number of terms incurs an approximation error $\leq 10^{-5}$. The fractal dimension D of both FBM and WMC functions is in one-to-one correspondence with H because $D = 2 - H$.

Some special methods (not covered in this paper due to their very narrow applicability) to measure D for FBM's include: i) Fitting a straight line to the data $(\log S(\omega), \log \omega)$ and measuring the slope yields H and hence D [12]. ii) The statistical self-affinity of FBM's yields a power scaling law for many of its moments; linear regression on these data can measure H and hence D [12]. iii) A maximum likelihood method for estimating the H of fractional Gaussian noise (derivatives of FBMs) was developed in [6]. (Note, that the spectral method (i) could also be applied to WMC's because their spectrum behaves like $1/\omega^{2H+1}$ too.)

2.3 Covering Method

In this paper we deal not with arbitrary curves but only with finite-length *signals* $f(t)$, $0 \leq t \leq T$, in which case the curve G of the previous discussion becomes the graph $G(f)$ of f. In this section we shall focus on a generalized version of the Minkowski cover method. That is, one generalized cover consistent with the definition of the "General Cover" method can be obtained as follows: given any *compact convex* planar set B, form positive homothetics $\epsilon B = \{\epsilon b : b \in B\}$, and define the cover $C(\epsilon)$ as the union of sets in $\mathcal{B}$, which contains all vector translates $\epsilon B + z = \{\epsilon b + z; b \in B\}$ of ϵB centered at points z of the graph $G(f)$. In the formalism of mathematical morphology this is equivalent to simply dilating $G(f)$ with a structuring element ϵB:

$$C(\epsilon) = \bigcup_{z \in G(f)} \epsilon B + z = G(f) \oplus \epsilon B \qquad (4)$$

Then (2) applies. The Minkowski cover method corresponds to using a disk for B. The "horizontal structuring element method" in [4] corresponds to using a line segment for B parallel to the domain of f.

In [4] the implementations of the Minkowski covering, box counting, and horizontal structuring methods were done by viewing $G(f)$ as a binary image signal and dilating this binary image. This, however, two-dimensional processing of a 1-dim signal, on the one hand is unneseccary and on the other hand squares the requirements in storage space and time complexity of implementing the covering method. Namely, let

$$\mathrm{Ypo}(f) = \{(t,y) \in \mathbf{R}^2 : y \leq f(t)\} \qquad (5)$$

be the *ypograph* of f (also known as "umbra" in morphology). Let also $(f \oplus g)(t) = \sup_x\{f(x) + g(t-x)\}$ and $(f \ominus g)(t) = \inf_x\{f(x) - g(x-t)\}$ be respectively the function *dilation* and *erosion* of f by a structuring function g with compact support. Then, (see [13,15,5,9] for properties of the ypographs), if we ignore the end effects around $t = 0$ and $t = T$, the dilated graph $C(\epsilon)$ can alternatively be obtained as the set difference between the ypographs of the dilated and eroded function; i.e., $C(\epsilon) \approx \mathrm{Ypo}(f \oplus \epsilon g) \setminus \mathrm{Ypo}(f \ominus \epsilon g)$, where g is such that

$$\mathrm{Ypo}(g) = \{(t,y) : y \leq b, (t,b) \in B\} . \qquad (6)$$

Further, $\mathrm{Ypo}(\epsilon g) = \epsilon \mathrm{Ypo}(g)$. Then, the cover area will be $A(\epsilon) \approx \int_0^T (f \oplus \epsilon g - f \ominus \epsilon g)(t)dt$. Thus, instead of creating the cover of a one-dimensional signal by expanding its graph in the plane (which means processing a two-dimensional signal), the original one-dimensional signal can be filtered with an erosion and a dilation system.

Putting all the above ideas together leads to what we shall henceforth call the *covering* method for estimating the fractal dimension of a discrete-argument finite-length signal $f[n]$, $n = 0, 1, \ldots, N$. This consists of the following steps:

1) Select a structuring function $g[n]$ with a 3-sample support (unit size) such that (6) is true, i.e., the graph of g is the upper boundary of B. B should be a unit-size discrete disk. For example, if B is a 5-pixel rhombus, then the structuring function is shaped like a *triangle*, defined by

$$g_t[-1] = g_t[1] = 0 , \; g_t[0] = h \geq 0, \; \text{and} \; g_t[n] = -\infty \; \forall n \neq -1, 0, 1. \qquad (7)$$

If B is the 3×3-pixel square, the corresponding structuring function is shaped like a *rectangle*:

$$g_r[n] = h \geq 0 \; n = -1, 0, 1, \; \text{and} \; g_r[n] = -\infty \; \forall n \neq -1, 0, 1. \qquad (8)$$

If $h = 0$, the structuring functions g_t and g_r become the same flat (binary) structuring element.

2) Perform the dilations and erosions of f by ϵg at discrete scales $\epsilon = 1, 2, \ldots, \epsilon_{max}$. For integer ϵ we define ϵ as the ϵ-fold dilation of g with itself. Then $f \oplus \epsilon g$ and $f \ominus \epsilon g$ can be implemented recursively:

$$f \oplus (\epsilon + 1)g = (f \oplus \epsilon g) \oplus g , \; f \ominus (\epsilon + 1)g = (f \ominus \epsilon g) \ominus g \qquad (9)$$

The dashed lines in Fig. 1a show these erosions/dilations by g_r at scales $\epsilon = 10, 20$.

3) Compute the areas $A[\epsilon] = \sum_{n=0}^{N}((f \oplus \epsilon g) - (f \ominus \epsilon g))[n]$.

4) Fit a straight line using least-squares linear regression to the plot of $(\log A[\epsilon]/\epsilon^2, \log 1/\epsilon)$. The slope of this line gives us the fractal dimension of f. For "real world" signals with some fractal structure, the assumption of exact self-similarity at all scales is not true. Hence, as in [11], instead of a global dimension, we estimate the *local fractal dimension* LFD(ϵ), which for each ϵ is equal to the slope of a line segment fitted to the log-log plot of (2) over a moving window $[\epsilon, \epsilon + 9]$ of 10 scales, where $\epsilon = 1, 2, ..., \epsilon_{max} - 9$.

Among previous approaches, the work in [11] and [14] (transposed to 1-dim signals) corresponds to using g_t with $h = 1$. The "horizontal structuring element method" in [4] corresponds to using $h = 0$.

Figure 1 shows results from experiments on evaluating the fractal dimension of FBM and WMC signals via the covering method using g_r with three different heights h. The shape of the structuring function g is not very crucial; g_t yields a slightly finer multiscale area distribution than g_r. The height h, however, plays an important role neglected by previous researchers. Although h does not affect the continuous version of the log-log plot (2), in the discrete case large h will sample this plot very coarsely and produce poor results. Thus small h are preferred for finer multiscale covering area distributions. However, the smaller h is, the more computations are needed to span a given signal's range. A good practical rule is to set h less than or equal to the signal's dynamic range divided by the number of its samples. This rule attempts to consider the quantization grid in the domain and range of the function as square as possible. Note that if $h = 0$, the erosions/dilations by g can be performed faster.

2.4 Variation Method

As Figs. 1b,1d show, even with a good selection of h, the covering method estimates for LFD(1) (i.e., the local fractal dimension for the first position of the scale window–first 10 scales) are not accurate. This is partly due to the quantization of the signal's domain and hence the small number of available samples to compute (at small scales) the local minima/maxima, as observed in [4]. Thus at $\epsilon = 1$ there is a neighborhood of only 3 samples for the min/max operations to create a cover. The *variation method* of Dubuc et al. [4] attempts to correct this problem by re-arranging the original signal samples $f[n]$, $0 \leq n \leq N$, to retain a smaller number of samples $0 \leq m \leq M \leq N$ and form the dilations $u_\epsilon[m]$ and erosions $b_\epsilon[m]$ at all scales ϵ, and by using essentially the covering method with a binary structuring function (i.e., $h = 0$) that has 3-sample domain for $\epsilon > 1$ and $2(N/M) + 1$-sample domain for $\epsilon = 1$. We have implemented the concept of the variation method in the following two different ways:

Variation by Signal Decimation: Let d be an integer variable decimation factor where $1 \leq d \leq d_{max} = \lfloor N/2\epsilon_{max} \rfloor$ and $\lfloor x \rfloor$ denotes the greatest integer $\leq x$. Erosion/dilation values are computed only every other d-th original sample. Thus, for $0 \leq m \leq M = \lfloor N/d \rfloor$,

$$
\begin{aligned}
u_1[m] &= \max\{f[n] : (m-1)d \leq n \leq (m+1)d\}, & \epsilon = 1 \\
u_\epsilon[m] &= \max(u_{\epsilon-1}[m-1], u_{\epsilon-1}[m+1]), & \epsilon = 2, 3, ..., \epsilon_{max}.
\end{aligned}
\tag{10}
$$

At the ends $m = 0, M$, the local max takes place only over the available samples. The erosions $b_\epsilon[m]$ are given from the formulae (10) by replacing max with min and u with b. The resulting LFD(ϵ) depends on d and hence on M. Two optimal values of d can be found by searching over all permissible values and finding that d which results in a better least-squares line fit to the log-log plot either over the *first* 10 scales or over *all* ϵ_{max} scales. Which of these two optimal values of d to use depends of course on the application.

Variation by Signal Truncation: Let $M + 1$ be the variable number of samples to retain after eliminating $N - M$ samples from the original signal f, where $2\epsilon_{max} = M_{min} \leq M \leq N$. Erosion/dilation values are computed only at $M + 1$ original samples. For each M, let $d = \lfloor N/M \rfloor$ be a integer ratio factor. Then $u_\epsilon[m]$ and $b_\epsilon[m]$ are computed for all ϵ exactly as for the variation by decimation method with d interpreted

now as a ratio rather than as a decimation factor. (Note that for several different M the integer d may remain the same.)

Figure 2 shows the results of estimating the LFD(ϵ) for FBM and WMC signals (with $D = 1.5$, $N = 500$, $e_{max} = 25$) by using both the variation by decimation and by truncation methods, which had similar performance. Both variation methods perform better than the covering method when an optimum d or M is selected. However, the variation by truncation is much more computionally intense than the decimation method. For example, with $N = 500$ and $e_{max} = 25$, the decimation method searches over $d = 1, .., 10$ and hence over 10 values of M, whereas the truncation method searches over all M with $50 \leq M \leq 500$. Note that the covering method with $h = 0$ becomes identical with the variation by decimation method if $d = 1$, and with the variation by truncation method if $M = N$.

3 Iterative Optimization Method

Assume a class of parametric fractal signals f_P parameterized by a parameter P that is related to their fractal dimension through an invertible function $D = \psi(P)$. For example, for FBM's or WMC's the parameter P is H and $D = \psi(H) = 2 - H$. Our new approach to measure the fractal dimension of such a signal f_P consists of the following steps: (1) We use a simple and fast morphological approach (i.e., the covering method with $h = 0$) to come up with an initial estimate, D^*, of the true D. (2) We compute some distance between the original fractal function f_P and another fractal f_{P*} which was synthesized to have dimension exactly $D^* = \psi(P^*)$. (3) By using nonlinear optimization, we search in the parameter space of P (or equivalently of D) values of the chosen class of fractals by synthesizing fractals whose parameters correspond to a fractal dimension D^* and computing their distances from the original fractal until this cycle converges to a local or global minimum in the parameter space. In this way the resulting fractal dimension will correspond to a fractal function which is also close (with respect to the specific distance) to the original function. We call this the *Iterative Optimization* method. As distance metrics we can use standard ℓ_p, $p = 1, 2, \infty$, metrics.

$$\ell_p(f_1, f_2) = ||f_1 - f_2||_p = \left(\sum_{n=-\infty}^{\infty} (f_1[n] - f_2[n])^p \right)^{\frac{1}{p}} \tag{11}$$

Further, we also introduce a definition of a Hausdorff metric for this iterative optimization. Our motivation for using this Hausdorff distance is that it is better suitable than ℓ_p distances to compare the geometrical structural differences (peak/valley distributions) between two signals in a way that agrees with human visual perception. The Hausdorff metric was so far defined only for sets. Here we extend its definition to functions and provide a morphological algorithm for its computation. Thus, given two compact sets A_1, A_2 their Hausdorff metric can be computed as

$$H(A_1, A_2) = \inf\{\epsilon : A_1 \subseteq A_2 \oplus \epsilon D \text{ and } A_2 \subseteq A_1 \oplus \epsilon D\}, \tag{12}$$

where ϵD is a disk of radius ϵ. If A_1 and A_2 become the ypographs of two functions f_1 and f_2 with compact supports, then we define their ypograph-based Hausdorff distance as

$$\text{Hy}(f_1, f_2) = H[\text{Ypo}(f_1), \text{Ypo}(f_2)] = \inf\{\epsilon : f_1 \leq f_2 \oplus \epsilon g \text{ and } f_2 \leq f_1 \oplus \epsilon g\} \tag{13}$$

Hy compares f_1 and f_2 in terms of their protrusions (peaks). If we want a distance sensitive both to the peaks and the valleys, then we can form the sum $\text{Hs}(f_1, f_2) = \text{Hy}(f_1, f_2) + \text{He}(f_1, f_2)$, which adds to $\text{Hy}(f_1, f_2)$ the Hausdorff distance $\text{He}(f_1, f_2) = \text{Hy}(c - f_1, c - f_2)$ of their epigraphs, i.e., of the negation-complements of f_1 and f_2 where c is some constant function.

Figure 3 reports a series of experiments whose goal was to inestigate how well can the Hausdorff or ℓ_p distances find a local/global minimum in comparing a given parametric fractal with an ensemble of similar fractals whose parameter varies over all possible values. Figs. 3a,3b,3e,3f show that both the Hy and the ℓ_1 distance yield a very clear global minimum when comparing an original FBM or WMC signal of a fixed D with similar signals whose D spans all the interval $[1,2]$. Resolutions of anywhere between 0.01 and 0.1 suffice to sample the parameter space of D and still observe a clear minimum. The Hy distance has a higher computational complexity than ℓ_1, and both yield similar results. For the Hy distance we used the structuring function g_r with $h = 0.01$. Using a smaller h or g_t instead of g_r refines Hy but requires more iterations of erosions/dilations. In Figs. 3a,3b the FBM's are viewed as deterministic functions (the random number generator was re-initialized for each D with the same seed). From a statistical viewpoint, however, they are random functions, and hence their Hausdorff and ℓ_p distances are actually random variables. Unfortunately, as Figs. 3c,3d show, the average Hy and ℓ_1 distances (the average was taken over 50 independent FBM realizations for each D) do not have a global minimum, except when $D > 0.5$ and the Hy distance is used (the Hs distance performs slightly better). Therefore, in our iterative optimization method, the FBM signals are viewed henceforth only deterministically. In all the above experiments we used both types of Hausdorff distances (Hy and Hs) and three types of ℓ_p distances ($p = 1, 2, \infty$). They all had similar performance for (deterministic) FBM and WMC signals. Hence we focus henceforth only on the Hy and the ℓ_1 distances.

Figure 4 compares the estimated local fractal dimension LFD(1) for FBM and WMC signals of varying dimension D and fixed duration $N = 500$ by using the covering, the variation by decimation, and our iterative optimization method. The iterative optimization was done by using the initial estimate from the covering method, and then improving it by first proceeding in the D space at steps of 0.01 and then (when in the neighborhood of the global minimum) by refining it with optimization steps of OS=0.001. As the Fig. 4 shows the iterative optimization method gives superior results than any other method since it achieves estimation errors that are practically zero for all D. (The errors are guaranteed to be in the order of OS; in our experiments, they were almost always in the order of 10^{-4} or 10^{-5}.) The ℓ_1 distance was used, but the Hy distance performed very similarly.

The same conclusions can be reached from Fig. 5 which shows the estimated dimension LFD(1) for FBM and WMC signals with varying duration N and fixed dimension D, by using all the previous approaches. Again, for all N the iterative optimization method outperforms all others and yields practically zero errors.

Comparing the covering and variation methods, we see from Figs. 4 and 5 that: 1) the covering method performs worse than the variation, except for very small $D < 1.2$ and small N. 2) In the variation method, optimizing the decimation factor d over the first 10 scales performs better than optimizing it over all scales for $D < 1.5$, whereas for $D > 1.5$ the opposite ir true. 3) Changing the signal length N affects the above conclusions for small $N < 300$.

4 An Application to Fractal Interpolation Functions

Given data points (x_i, y_i), $i = 0, 1, .., I$, we are concerned with continuous functions $f : S \to \mathbf{R}$ on a compact interval S, which interpolate the data as $f(x_i) = y_i$ and whose graphs are attractors of Iterated Function Systems (IFS) [1]. These systems consist of a finite number of affine contractive maps which can model well self-similar sets as the union (collage) of small patches (each patch is the transformation of the original set by an affine map). A general affine map for an IFS is

$$w_n \begin{pmatrix} x \\ y \end{pmatrix} = \begin{bmatrix} a_n & b_n \\ c_n & d_n \end{bmatrix} \begin{bmatrix} x \\ y \end{bmatrix} + \begin{bmatrix} e_n \\ f_n \end{bmatrix} \ , \quad n = 1, 2, \ldots, I. \tag{14}$$

We have a finite number I of such maps, each associated with some probability p_n. If the maps are contractive, then there exists a random algorithm [1] in which a point (x, y) is iteratively mapped to other points by these affine maps (randomly chosen with probability p_n) and thus fills the points of a unique attractor. For such an IFS to have as attractor the graph of a function its parameters must have some restrictions. Namely, for the n-th affine map,

$$
\begin{aligned}
a_n &= (x_n - x_{n-1})/(x_I - x_0) \ , \quad b_n = 0 \ , \quad e_n = x_{n-1} - a_n x_0. \\
d_n &\in (-1, 1) \ , \quad c_n = [y_n - y_{n-1} - d_n(y_I - y_0)]/(x_I - x_0) \ , \quad f_n = y_{n-1} - d_n y_0 - c_n x_0.
\end{aligned}
\tag{15}
$$

Here we assume that $d_n = V$ is constant for all n, and we call it the "vertical scale parameter" (contraction factor) V. Thus given the initial data points (x_i, y_i), the *fractal interpolated function (FIF)* f_V is a unique fractal signal parameterized by V. Figure 6a shows an original function f (an FBM of 256 points with $H = 0.3$). As data (x_i, y_i) we select 17 points from this function f, whose x_i are equally spaced; hence all $a_n = 1/16$. Figs. 6b,6c show two signals that resulted from the IFS interpolation algorithm with $V = -0.6, +0.6$; the dotted line shows the piecewise linear interpolation between the original 17 points. The larger the V, the rougher looks the interpolated function f_V. All these interpolated functions were computed at $I_{int} = 256$ sample points equally spaced in their domain. Fig. 6d shows the fractal dimension LFD(1) (computed using the covering method with g_r and $h = 0.01$) of f_V for V spanning the interval [-0.9,0.7] at steps of 0.032. We see that the relation between V and the fractal dimension D is one-to-one over each half of the V parameter space (-1,1). (We are currently working to provide an approximate analytic formula for this relation.) Figs 6e and 6f show, respectively, the Hausdorff and ℓ_p distances (mean absolute error, rms error, and max absolute error) between the original f and the interpolated f_V, as a function of the parameter V. Selecting one local minimum for the symmetric Hausdorff distance gives us $V = -0.8$, whereas the minimum for the ℓ_∞ distance gives us $V = -0.1$. Plotting the corresponding interpolated functions in Figs. 6g and 6h shows that the optimal parameter V extracted via the Hausdorff-distance minimization approximates f with an interpolated function that is closer to f in a way that agrees more with the human perception of the roughness of the function's graph.

Finally instead of searching through the whole parameter space V, we can instead find first the fractal dimension which will give us an initial estimate of V, due to the one-to-one relation between D and V, and then improve this initial estimate by searching locally around it.

References

[1] M. F. Barnsley, "Fractal Interpolation Functions", *Constr. Approx.*, 2, pp. 303-329, 1986.

[2] M. V. Berry and Z. V. Lewis, "On the Weierstrass-Mandelbrot fractal function", *Proc. R. Soc. Lond. A*, 370, pp.459-484, 1980.

[3] G. Bouligand, "Sur la notion d'ordre de mesure d'un ensemble plan", *Bull. Sci. Math.*, II-53, pp.185-192, 1929.

[4] B. Dubuc, J. F. Quiniou, C. Roques-Carmes, C. Tricot and S. W. Zucker, "Evaluating the fractal dimension of profiles", *Phys. Rev. A*, vol.39, pp.1500-1512, Feb. 1989.

[5] R. M. Haralick, S. R. Sternberg, and X. Zhuang, "Image Analysis Using Mathematical Morphology", *IEEE Trans. Pattern Anal. Mach. Intell.*, PAMI-9, pp.523-550, July 1987.

[6] T. Lundahl, W.J. Ohley, S.M. Kay, and R. Siffert, "Fractional Brownian Motion: A Maximum Likelihood Estimator and Its Application to Image Texture", *IEEE Trans. Med. Imag.*, MI-5, pp.152-160, Sep. 1986.

[7] B. B. Mandelbrot, *The Fractal Geometry of Nature*, NY: W.H. Freeman, 1982,1983.

[8] B. B. Mandelbrot and J. van Ness, "Fractional Brownian motion, fractional noise and applications", *SIAM Review*, 10(4), pp. 422-437, 1968.

[9] P. Maragos and R. W. Schafer, "Morphological Filters - Part I: Their Set-Theoretic Analysis and Relations to Linear Shift-Invariant Filters," *IEEE Trans. Acoust. Speech, Signal Processing*, pp.1153-1169, Aug. 1987.

[10] H. Minkowski, "Uber die Begriffe Lange, Oberflache und Volumen", *Jahresber. Deutch. Mathematik-erverein.*, 9, pp. 115-121, 1901.

[11] S. Peleg, J. Naor, R. Hartley and D. Avnir, "Multiple Resolution Texture Analysis and Classification", *IEEE Trans. Pattern. Anal. Mach. Intell.*, PAMI-6, pp.518-523, July 1984.

[12] A. P. Pentland, "Fractal-Based Description of Natural Scenes", *IEEE Trans. Pattern Anal. Mach. Intell.*, PAMI-6, pp. 661-674, Nov. 1984.

[13] J. Serra, *Image Analysis and Mathematical Morphology*, NY: Acad. Press, 1982.

[14] M. C. Stein, "Fractal image models and object detection", in *Proc. SPIE 845: Visual Communications and Image Processing II*, 1987.

[15] S. R. Sternberg, "Grayscale Morphology," *Comput. Vision, Graph., Image Proc.* **35**, pp.333-355, 1986.

[16] C. Tricot, J. Quiniou, D. Wehbi, C. Roques-Carmes, et B. Dubuc, "Evaluation de la dimension fractale d'un graphe", *Revue Phys. Appl.*, 23, pp.111-124, 1988.

[17] R. F. Voss, "Fractals in nature: From characterization to simulation", in *The Science of Fractal Images*, H.-O. Peitgen and D. Saupe, Eds, Springer-Verlag, 1988.
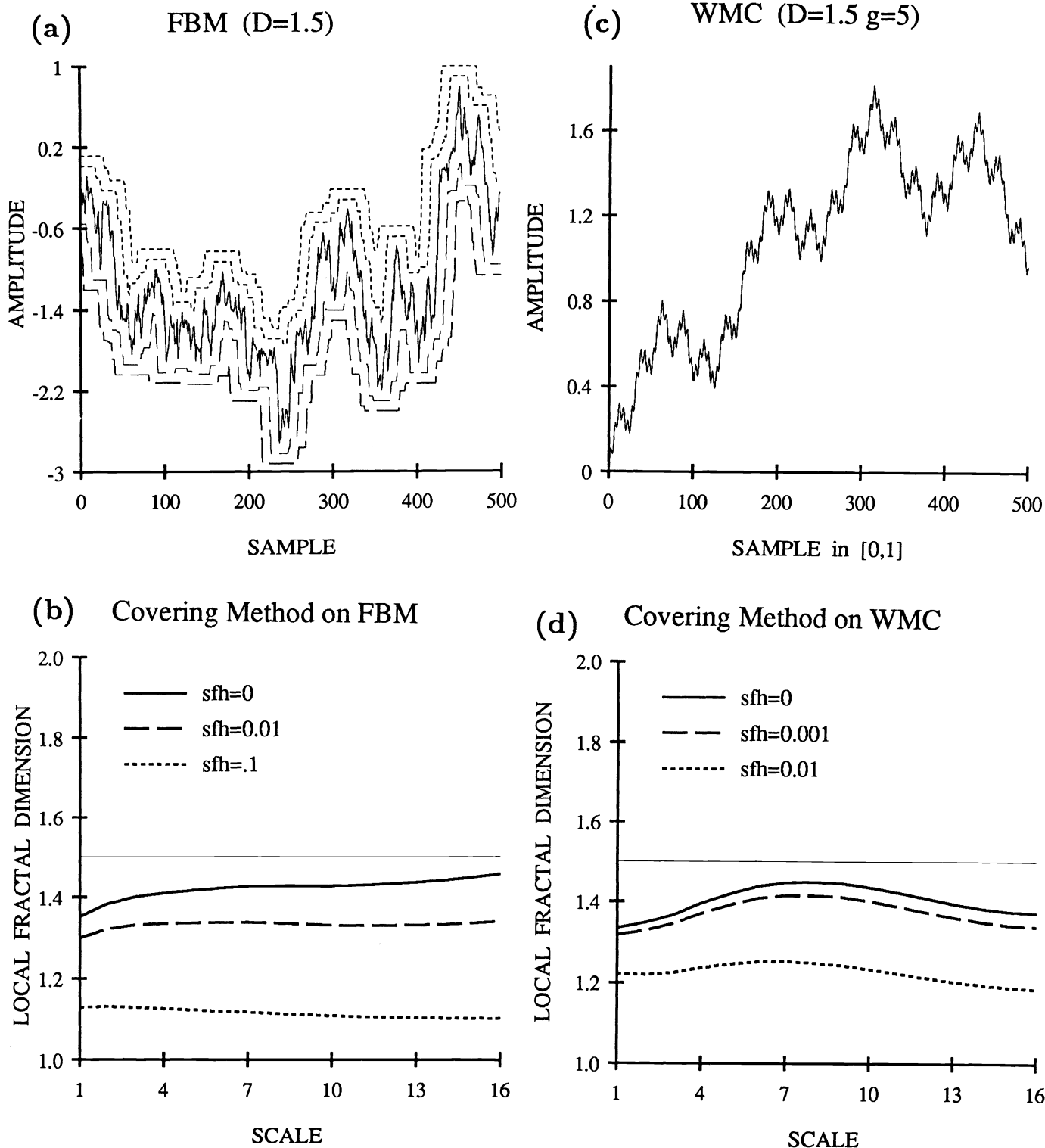
FIGURE 1. (a) An FBM function (solid line) with $H = 0.5$, $N = 500$ and its erosions/dilations (dashed lines) by ϵg_r ($\epsilon = 10, 20$, $h = 0.01$). (b) Estimation of LFD of FBM via the covering method using g_r with 3 different heights $h = 0, 0.01, 0.1$ ($\epsilon_{max} = 25$). (The thin solid straight line shows the true $D = 1.5$.) (c) and (d) same as (a) and (b) but for a WMC function and with $h = 0, 0.001, 0.01$.
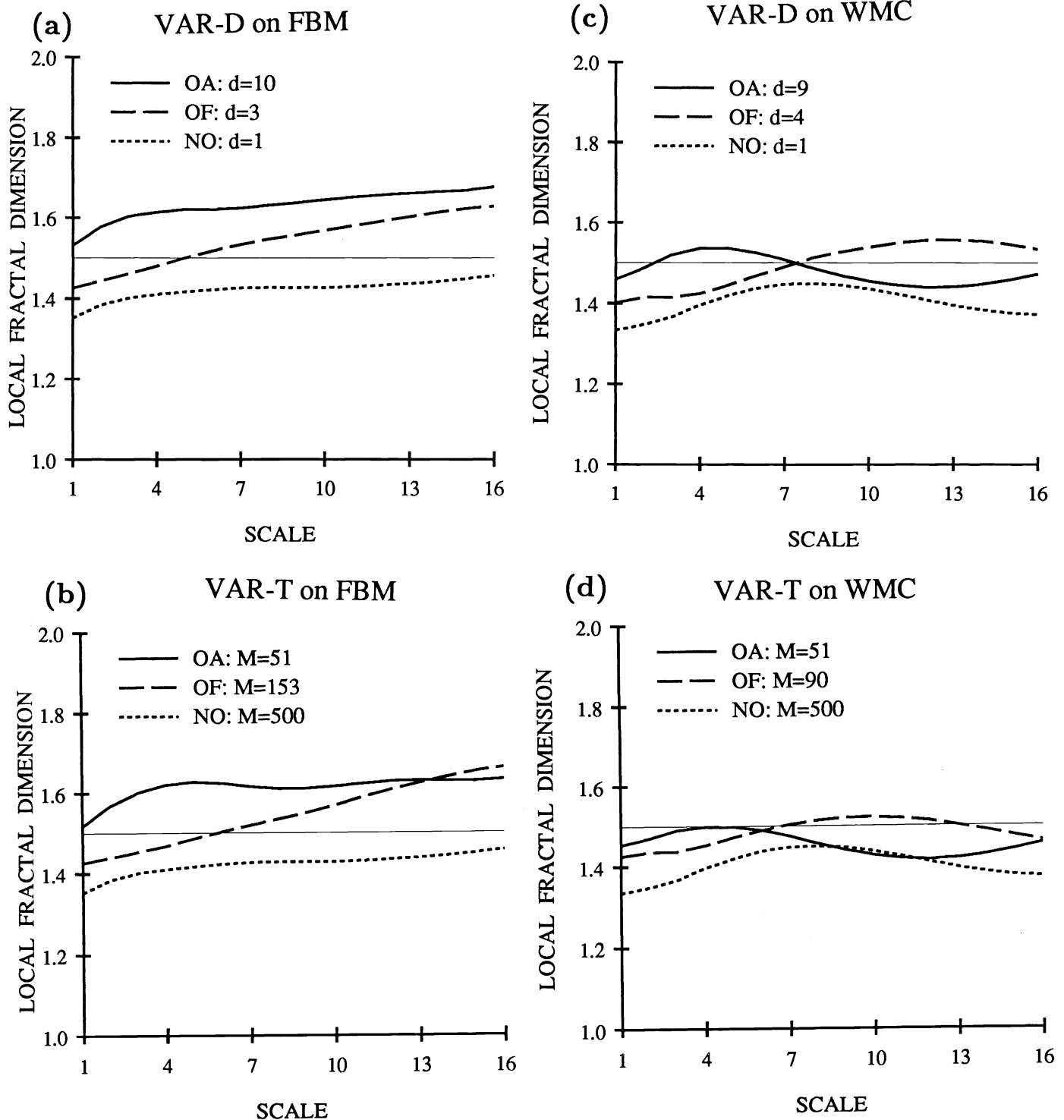
FIGURE 2. (a) Estimation of LFD of an FBM function ($H = 0.5, N = 500$) via the variation by *decimation* method. The thin solid line shows the true $D = 1.5$. The OA and OF lines show the estimates resulted from optimizing the decimation factor d over *all* $e_{max} = 25$ scales or over the *first* 10 scales, respectively. The NO line corresponds to not optimizing and not decimating ($d = 1$). (b) same as in (a) but using the variation by *truncation* method. (The NO line corresponds to not truncating since $M = N = 500$.) (c) and (d) same as (a) and (b) but for a WMC function.
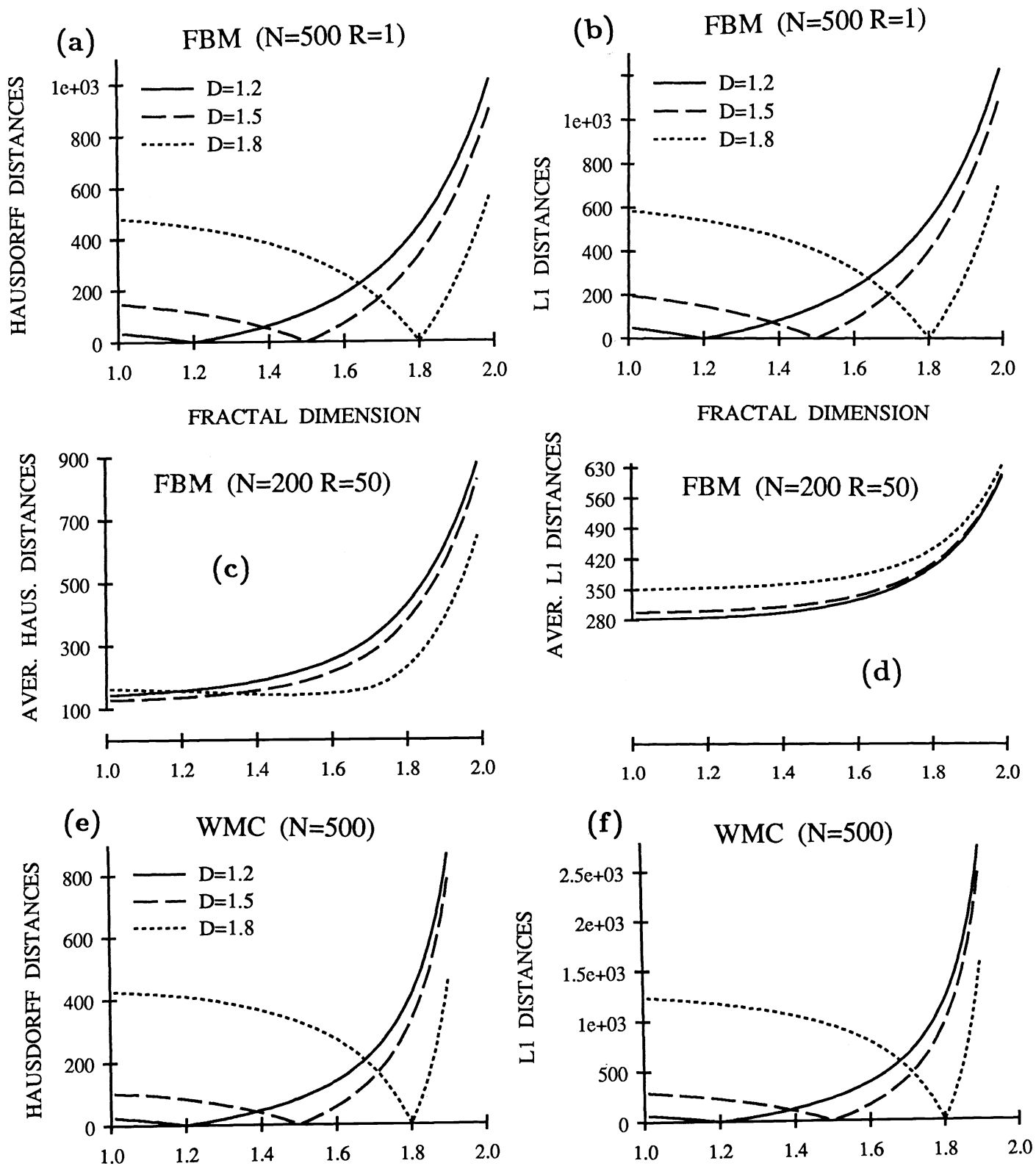
FIGURE 3. (a) Hausdorff distances $Hy(f_i, f_D)$ between three fixed FBM functions f_i with $D_i = 1.2, 1.5, 1.8$ and variable FBM functions f_D whose D spans the interval [1.01,1.99] at steps of 0.01. (b) same as (a) but using $\ell_1(f_i, f_D)$ distances. (c) and (d) are same as (a) and (b) but the distances are averaged over 50 realizations of the FBM f_D for each D. (e) and (f) are same as (a) and (b) but for WMC functions.
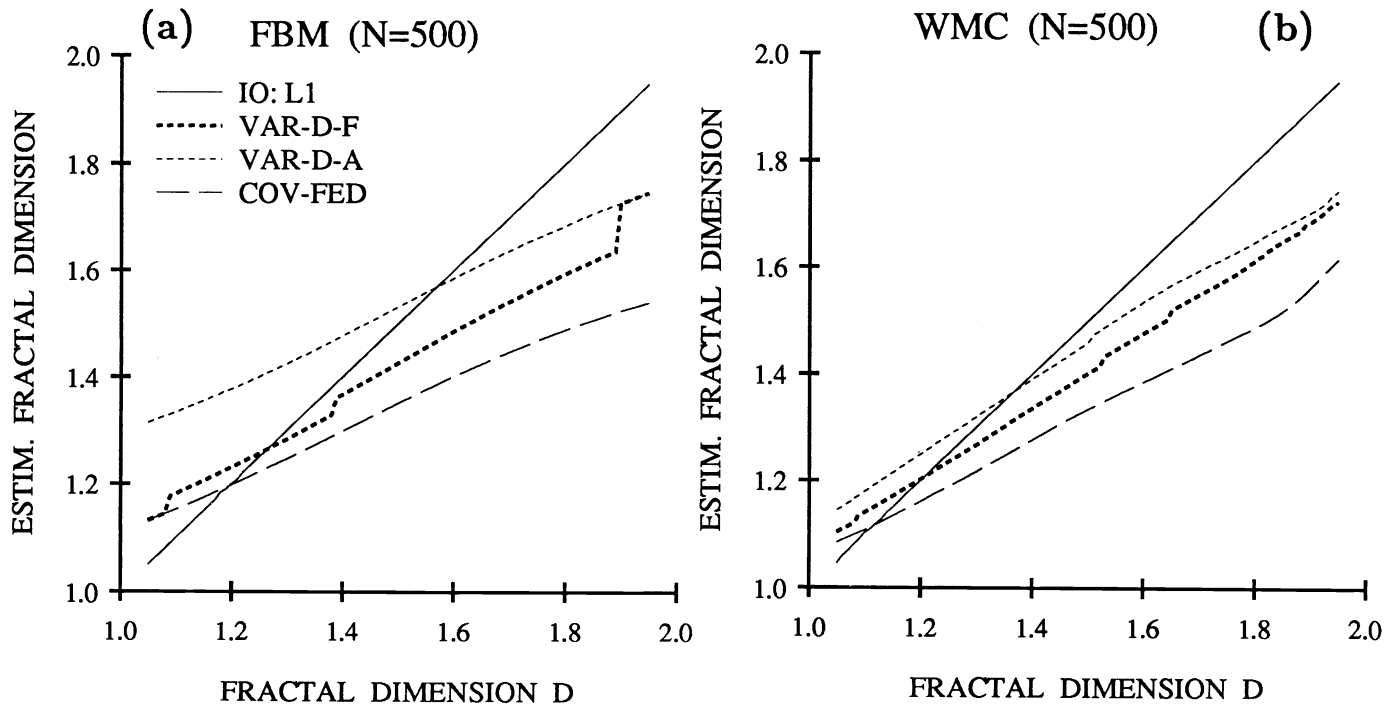
FIGURE 4. Estimating the LFD(1) of [FBM in (a) and WMC in (b)] signals whose D spans the interval [1.05,1.95] at steps of 0.01. The IO line corresponds to the iterative optimization method using the ℓ_1 distance. The VAR-D-A and VAR-D-F lines correspond to the variation by decimation method where the decimation factor is optimized over all $\epsilon_{max} = 25$ scales or over the first 10 scales, respectively. The COV-FED line correponds to the covering method with g_r and $h = 0$.
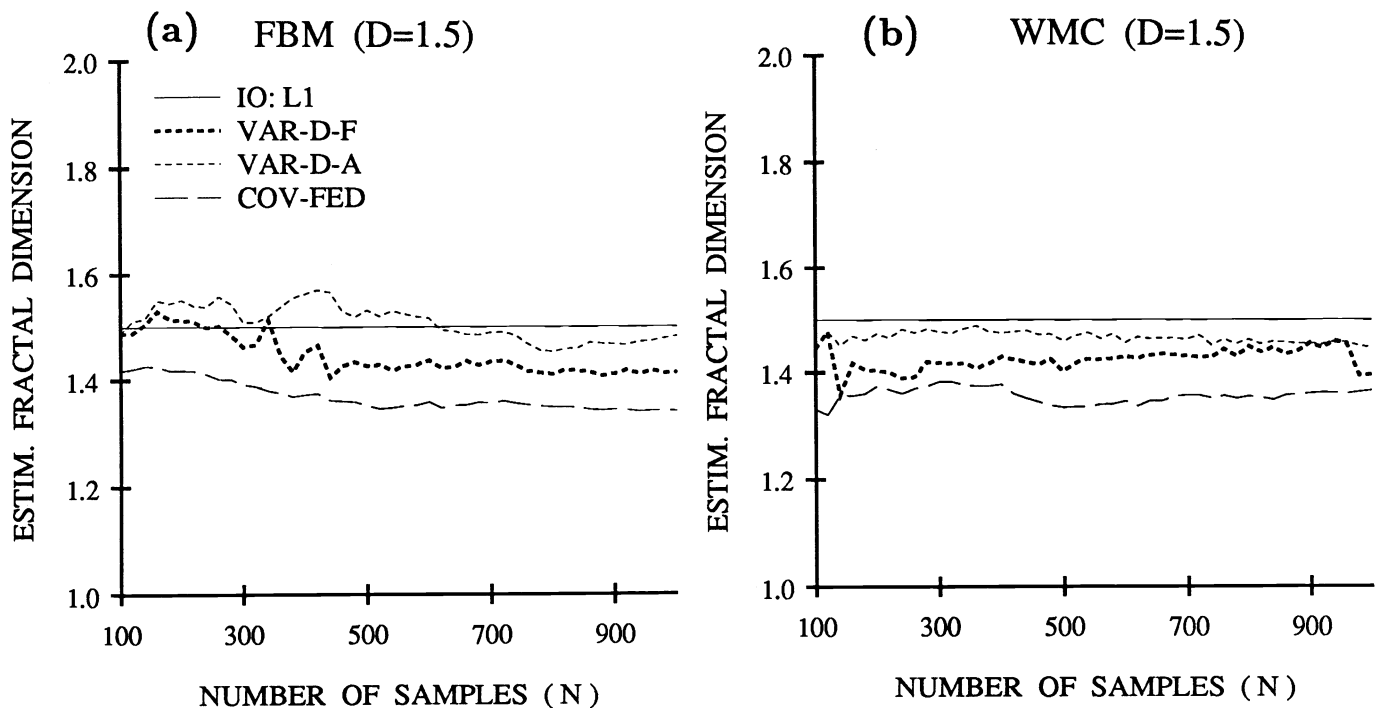
FIGURE 5. Estimates of the fractal dimension LFD(1) of [FBM in (a) and WMC in (b)] signals with $D = 1.5$ and N spanning the interval [100,1000] at steps of 20. The line identities are as in Fig. 4.

(c) FBM (D=1.3)

(d) WMC (D=1.3)

(e) FBM (D=1.8)

(f) WMC (D=1.8)

Legend (for each plot):
IO: L1
VAR-D-F
VAR-D-A
COV-FED

Axis labels: ESTIM. FRACTAL DIMENSION (vertical), NUMBER OF SAMPLES (N) (horizontal)
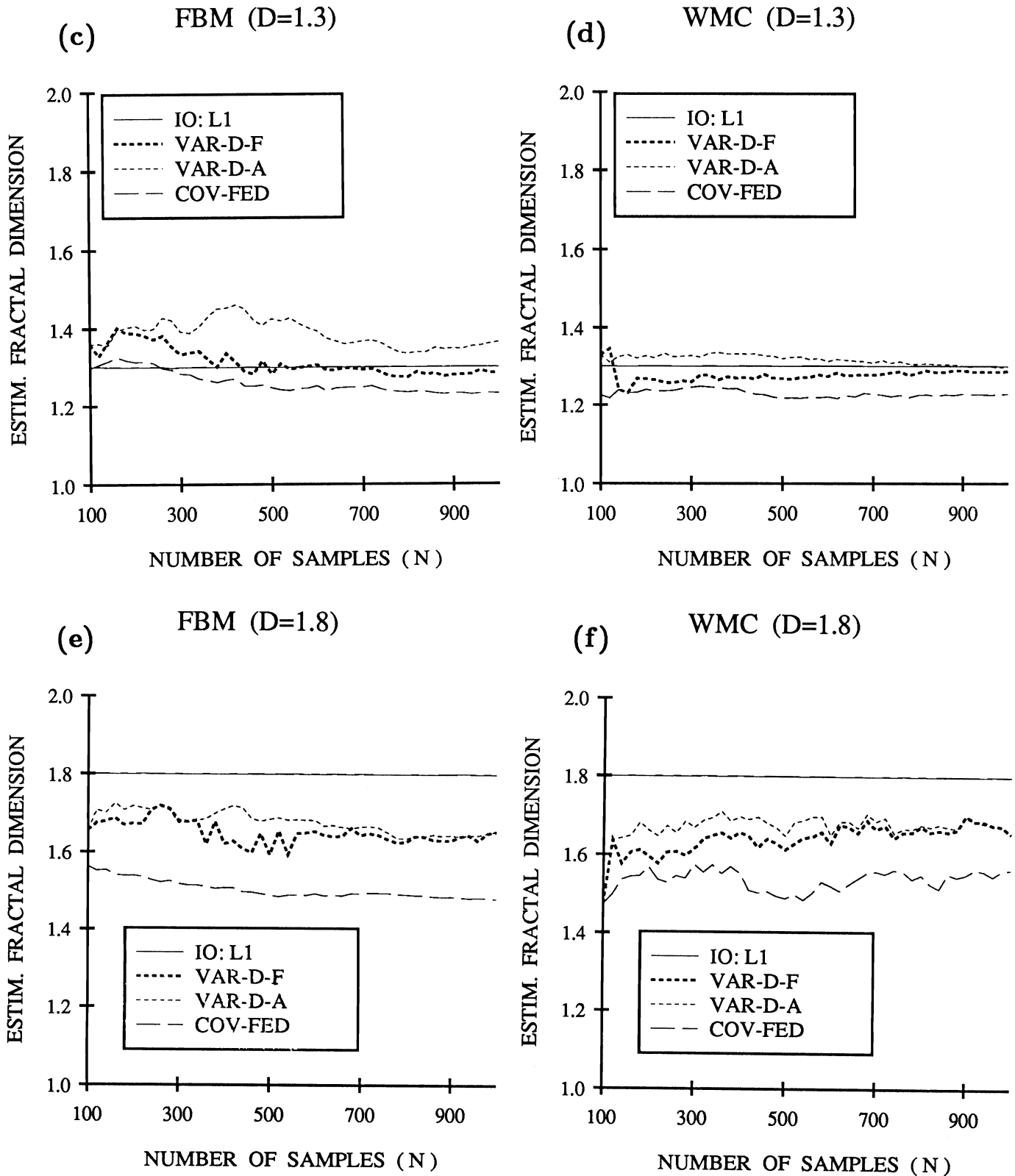
FIGURE 5 (cont'd). (c) and (d) are same as (a) and (b) but with $D = 1.3$. (e) and (f) are same as (a) and (b) but with $D = 1.8$.
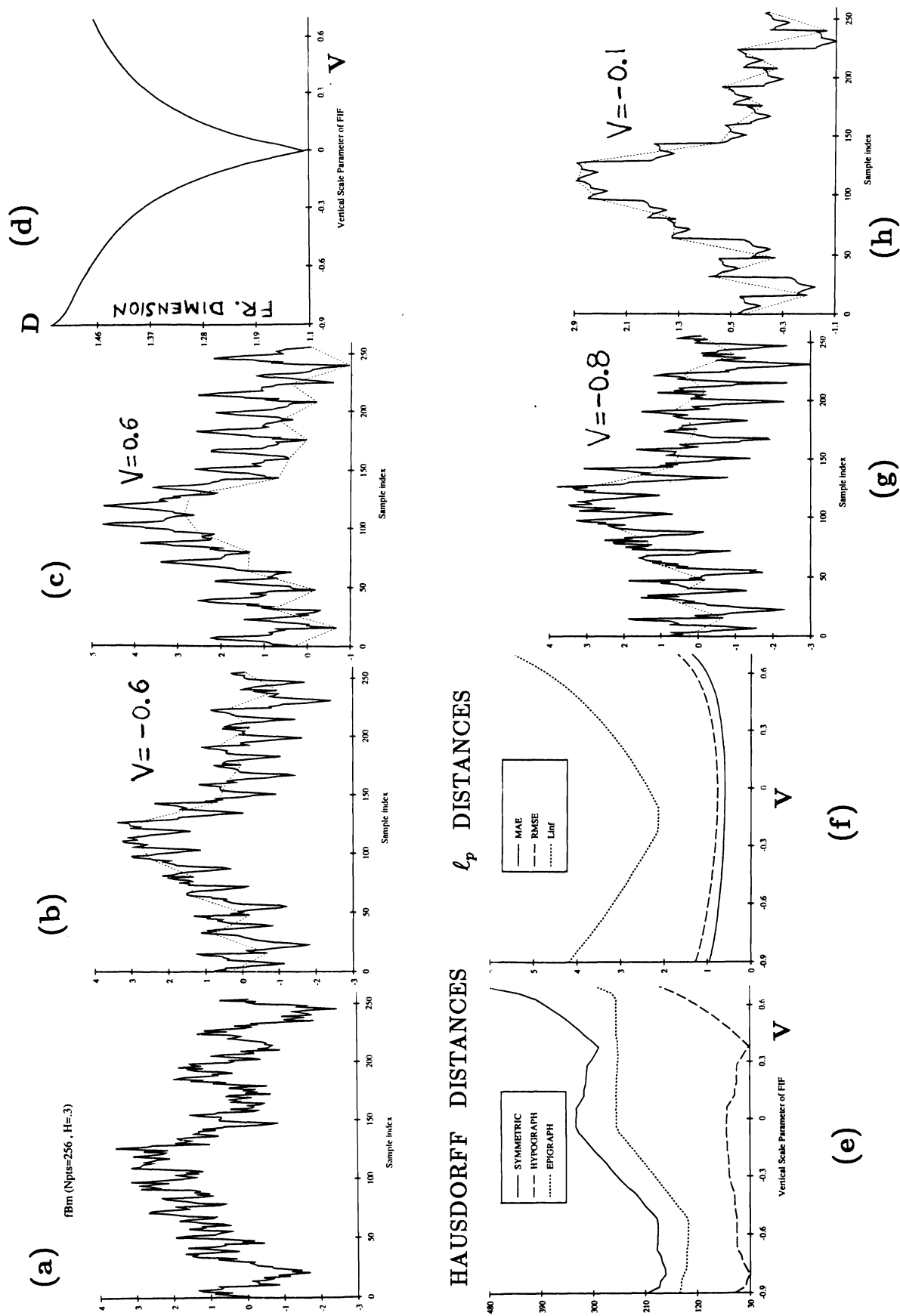
FIGURE 6. (a) Original 256-sample FBM function f with $H = 0.3$. (b) Synthesized FIF with $V = -0.6$. (c) FIF with $V = 0.6$. (d) Fractal dimension of FIFs f_V with varying V. (e) Hausdorff distances between f and all f_V. (f) ℓ_p distances between f and all f_V. (g) FIF with $V = -0.8$. (h) FIF with $V = -0.1$.